

## Calculations of optical properties in strongly correlated materials

V. S. Oudovenko,<sup>1,2</sup> G. Pálsson,<sup>2</sup> S. Y. Savrasov,<sup>3</sup> K. Haule,<sup>2</sup> and G. Kotliar<sup>2</sup>

<sup>1</sup>*Bogoliubov Laboratory for Theoretical Physics, Joint Institute for Nuclear Research, 141980 Dubna, Russia*

<sup>2</sup>*Center for Materials Theory, Department of Physics and Astronomy, Rutgers University, Piscataway, New Jersey 08854, USA*

<sup>3</sup>*Department of Physics, New Jersey Institute of Technology, Newark, New Jersey 07102, USA*

(Received 30 March 2004; published 24 September 2004)

We present a method to calculate optical properties of strongly correlated systems. It is based on dynamical mean-field theory and it uses as an input realistic electronic structure obtained by local density-functional calculations. Numerically, tractable equations for optical conductivity, which show a correct noninteracting limit, are derived. Illustration of the method is given by computing optical properties of the doped Mott insulator  $\text{La}_{1-x}\text{Sr}_x\text{TiO}_3$ .

DOI: 10.1103/PhysRevB.70.125112

PACS number(s): 71.20.-b, 71.27.+a, 78.20.-e

### I. INTRODUCTION

Optical spectral functions such as conductivity or reflectivity are very important characteristics of solids, which give us a direct probe of their electronic structure. In the past, very powerful numerical techniques<sup>1</sup> based on density-functional theory (DFT) and local-density approximation (LDA) have been developed, which allowed to access the one-electron spectrum in real materials via association of LDA energy bands with the real excitation energies. This approach works well for weakly correlated systems, where, for example, optical properties can be directly computed<sup>2</sup> via the knowledge of the band structure and the dipole matrix elements of the material. Furthermore, for weakly correlated materials LDA is a good starting point for adding perturbative corrections in the screened Coulomb interactions following the *GW* approach.<sup>3</sup>

Unfortunately, the treatment of materials with strong electronic correlations is not possible within this framework. Strong on-site Coulomb repulsion modifies the one-electron spectrum via appearance of satellites, Hubbard bands, strongly renormalized Kondo-like states, etc., which are no longer obtainable using static mean-field theories such as Hartree-Fock theory or LDA. The wave functions in strongly correlated systems are not representable by single Slater determinants and dynamical self-energy effects become important, thus requiring a new theoretical treatment based on the dynamical mean-field theory (DMFT).<sup>4</sup> Recent advances<sup>5</sup> in merging the DMFT with realistic LDA based electronic structure calculations have already led to solving such long-standing problems as, e.g., temperature-dependent magnetism of Fe and Ni,<sup>6</sup> volume collapse in Ce,<sup>7</sup> and huge volume expansion of Pu.<sup>8</sup>

In the present work we develop an approach which allows us to calculate the optical properties of strongly correlated materials within the combined LDA and DMFT framework. We discuss the expressions for optical conductivity using self-energies and local Green's functions, which are numerically tractable and correctly reproduce the limit of noninteracting electrons. We also check the limit of strong correlations by applying the method to three-band Hubbard Hamiltonian. Results of this test reproduce the available experimental and theoretical data with very good accuracy. We

demonstrate the applicability of the present scheme on the example of doped Mott insulator  $\text{La}_{1-x}\text{Sr}_x\text{TiO}_3$ , where we compare the results of our calculations with the LDA predictions and experiment.

The paper is organized as follows. In Sec. II we describe the method for calculation of the optical conductivity. Application of the method to doped  $\text{La}_{1-x}\text{Sr}_x\text{TiO}_3$  is described and analyzed in Sec. III, which is followed by conclusions presented in Sec. IV. Some technical details of the calculations and the downfolding and upfolding procedures are given in the Appendix.

### II. METHOD

To calculate the optical response functions we utilize the dynamical mean-field approach where the self-energy of the many-body problem is approximated by a local operator  $\Sigma(\omega)$  which is, however, frequency dependent. A physical transparent description of this method can be achieved by introducing an interacting analog of Kohn-Sham particles,  $\psi_{\mathbf{k}j}(\mathbf{r}, \omega) \equiv \psi_{\mathbf{k}j\omega}$ , which reproduce the local portion of the Green's function in a similar way as the noninteracting Kohn-Sham particles  $\psi_{\mathbf{k}j}(\mathbf{r})$  reproduce the density of the solid in its ground state. This spectral density-functional approach<sup>9</sup> has an advantage that the  $\mathbf{k}$ -integrated excitation properties (such as, e.g., densities of states) can now be associated with the real one-electron spectra. The optical transitions between the interacting quasiparticles  $\psi_{\mathbf{k}j\omega}$  allow the excitations between incoherent and coherent parts of the spectra (e.g., between Hubbard and quasiparticle bands) which are intrinsically missing in static mean-field approaches such as DFT but are present in real strongly correlated situations.

In order to find the quasiparticles living at a given frequency  $\omega$  we solve the Dyson equation with the LDA potential  $V_{\text{eff}}$  and the frequency-dependent correction  $\Sigma(\omega) - \Sigma_{dc}$ , i.e.,

$$[(-\nabla^2 + V_{\text{eff}} + \Sigma(\omega) - \Sigma_{dc} - \epsilon_{\mathbf{k}j\omega})]\psi_{\mathbf{k}j\omega}^R = 0. \quad (1)$$

A double-counting term  $\Sigma_{dc}$  appears here to account for the fact that  $V_{\text{eff}}$  is the average field which acts on both heavy

(localized) and light (itinerant) electrons. Note that due to the non-Hermitian nature of the problem, both “right”  $\psi^R$  and “left”  $\psi^L$  eigenvectors should be considered, the latter being the solution of the same Dyson equation (1) with  $\psi$  placed on the left. The local Green’s function is constructed from the eigenvectors and eigenvalues in the following way:

$$G(\omega) = \sum_{\mathbf{k}j} \frac{\psi_{\mathbf{k}j\omega}^R \psi_{\mathbf{k}j\omega}^L}{\omega + \mu - \epsilon_{\mathbf{k}j\omega}}. \quad (2)$$

The local self-energy is calculated from the corresponding impurity problem which is defined by the DMFT self-consistency condition

$$G(\omega) = [\omega - E_{imp} - \Sigma(\omega) - \Delta_{imp}(\omega)]^{-1}, \quad (3)$$

where  $\Delta_{imp}$  is the impurity hybridization matrix and  $E_{imp}$  are the impurity levels. From known  $\Delta_{imp}(\omega)$ ,  $E_{imp}$ , and Coulomb interaction  $U$ , the solution of the Anderson impurity problem then delivers the local self-energy  $\Sigma(\omega)$ . The system of equations (1)–(3), together with an impurity solver, i.e., a functional  $\Sigma[\Delta_{imp}(\omega), E_{imp}, U]$ , is thus closed.

Solution of the Anderson impurity model can be carried out by available many-body technique<sup>4</sup> such as the quantum Monte Carlo (QMC) method<sup>10</sup> which will be used in our work. In practice,<sup>5,8</sup> we utilize the LDA+DMFT approximation and treat only the  $d$  electrons of Ti as strongly correlated, thus requiring full energy resolution. All other electrons are assumed to be well described by the LDA. The Dyson equation is solved on the Matsubara axis for a finite set of imaginary frequencies  $i\omega_n$  using a localized orbital representation such as, e.g., linear muffin-tin orbitals (LMTO’s)<sup>11</sup> for the eigenvectors  $\psi_{\mathbf{k}j\omega}$ .

The optical conductivity can be expressed via equilibrium state current-current correlation function<sup>12</sup> and is given by

$$\begin{aligned} \sigma_{\mu\nu}(\omega) &= \pi e^2 \int_{-\infty}^{+\infty} d\varepsilon \phi_{\mu\nu}(\varepsilon + \omega/2, \varepsilon - \omega/2) \\ &\times \frac{f(\varepsilon - \omega/2) - f(\varepsilon + \omega/2)}{\omega}, \end{aligned} \quad (4)$$

where  $e$  is free electron charge,  $f(\varepsilon)$  is the Fermi function, and the transport function  $\phi_{\mu\nu}(\varepsilon, \varepsilon')$  is defined as

$$\phi_{\mu\nu}(\varepsilon, \varepsilon') = \frac{1}{\mathcal{V}} \sum_{\mathbf{k}jj'} \text{Tr}\{\nabla_{\mu} \hat{\rho}_{\mathbf{k}j}(\varepsilon) \nabla_{\nu} \rho_{\mathbf{k}j'}(\varepsilon')\}, \quad (5)$$

with  $\mathcal{V}$  being the unit-cell volume and

$$\rho_{\mathbf{k}j}(\varepsilon) = -\frac{1}{2\pi i} [G_{\mathbf{k}j}(\varepsilon) - G_{\mathbf{k}j}^{\dagger}(\varepsilon)] \quad (6)$$

is expressed via retarded one-particle Green’s function  $G_{\mathbf{k}j}(\varepsilon)$ . Using the solutions  $\epsilon_{\mathbf{k}j\omega}$  and  $\psi_{\mathbf{k}j\omega}$  of the Dyson equation (1) we express the optical conductivity in the form

$$\begin{aligned} \sigma_{\mu\nu}(\omega) &= -\frac{e^2}{4\pi} \sum_{ss'=\pm 1} ss' \sum_{\mathbf{k}jj'} \int_{-\infty}^{+\infty} d\varepsilon \frac{M_{\mathbf{k}jj'}^{ss',\mu\nu}(\varepsilon^-, \varepsilon^+)}{\omega + \epsilon_{\mathbf{k}j\varepsilon^-}^s - \epsilon_{\mathbf{k}j'\varepsilon^+}^{s'}} \\ &\times \left[ \frac{1}{\varepsilon^- + \mu - \epsilon_{\mathbf{k}j\varepsilon^-}^s} - \frac{1}{\varepsilon^+ + \mu - \epsilon_{\mathbf{k}j'\varepsilon^+}^{s'}} \right] \frac{f(\varepsilon^-) - f(\varepsilon^+)}{\omega}, \end{aligned} \quad (7)$$

where we have denoted  $\varepsilon^{\pm} = \varepsilon \pm \omega/2$ , and used the shortcut notations  $\epsilon_{\mathbf{k}j\varepsilon}^+ \equiv \epsilon_{\mathbf{k}j\varepsilon}$ ,  $\epsilon_{\mathbf{k}j\varepsilon}^- \equiv \epsilon_{\mathbf{k}j\varepsilon}^*$ .

The matrix elements  $M_{\mathbf{k}jj'}$  are generalizations of the standard dipole allowed transition probabilities which are now defined with the right and left solutions  $\psi^R$  and  $\psi^L$  of the Dyson equation:

$$\begin{aligned} M_{\mathbf{k}jj'}^{ss',\mu\nu}(\varepsilon, \varepsilon') &= \int (\psi_{\mathbf{k}j\varepsilon}^s)^s \nabla_{\mu} (\psi_{\mathbf{k}j'\varepsilon'}^{s'})^{s'} d\mathbf{r} \\ &\times \int (\psi_{\mathbf{k}j'\varepsilon'}^{s'})^{s'} \nabla_{\nu} (\psi_{\mathbf{k}j\varepsilon}^s)^s d\mathbf{r}, \end{aligned} \quad (8)$$

where we denoted  $\psi_{\mathbf{k}j\varepsilon}^+ = \psi_{\mathbf{k}j\varepsilon}^L$ ,  $\psi_{\mathbf{k}j\varepsilon}^- = \psi_{\mathbf{k}j\varepsilon}^R$  and assumed that  $(\psi_{\mathbf{k}j\varepsilon}^s)^+ \equiv \psi_{\mathbf{k}j\varepsilon}^s$  and  $(\psi_{\mathbf{k}j\varepsilon}^s)^- \equiv \psi_{\mathbf{k}j\varepsilon}^{s*}$ . Expressions (7) and (8) represent generalization of the optical conductivity formula for the case of strongly correlated systems, and involve the extra internal frequency integral appearing in Eq. (7).

Let us consider the noninteracting limit when  $\Sigma(\omega) - \Sigma_{dc} \rightarrow i\gamma \rightarrow 0$ . In this case, the eigenvalues  $\epsilon_{\mathbf{k}j\varepsilon} = \epsilon_{\mathbf{k}j} + i\gamma$ ,  $\psi_{\mathbf{k}j\varepsilon}^R \equiv |\mathbf{k}j\rangle$ ,  $\psi_{\mathbf{k}j\varepsilon}^L \equiv |\mathbf{k}j\rangle^* \equiv \langle \mathbf{k}j|$  and the matrix elements  $M_{\mathbf{k}jj'}^{ss',\mu\nu}(\varepsilon, \varepsilon')$  are all expressed via the standard dipole transitions  $|\langle \mathbf{k}j|\nabla|\mathbf{k}j'\rangle|^2$ . Working out the energy denominators in expression (7) in the limit  $i\gamma \rightarrow 0$  and for  $\omega \neq 0$  leads us to the usual form for the conductivity which for its interband contribution can be written as

$$\begin{aligned} \sigma_{\mu\nu}(\omega) &= \frac{\pi e^2}{\omega} \sum_{\mathbf{k}, j' \neq j} \langle \mathbf{k}j|\nabla_{\mu}|\mathbf{k}j'\rangle \langle \mathbf{k}j'|\nabla_{\nu}|\mathbf{k}j\rangle \\ &\times [f(\epsilon_{\mathbf{k}j}) - f(\epsilon_{\mathbf{k}j'})] \delta(\epsilon_{\mathbf{k}j} - \epsilon_{\mathbf{k}j'} + \omega). \end{aligned} \quad (9)$$

To evaluate the expression  $\sigma_{\mu\nu}(\omega)$  in Eq. (7) numerically, we need to perform integration over  $\varepsilon$  and pay a special attention to the energy denominator  $1/(\omega + \epsilon_{\mathbf{k}j\varepsilon}^s - \epsilon_{\mathbf{k}j'\varepsilon^+}^{s'})$ . To calculate the integral over  $\varepsilon$  we divide frequency domain into discrete set of points  $\varepsilon_i$  and assume that the eigenvalues  $\epsilon_{\mathbf{k}j\varepsilon}$  and eigenvectors  $\psi_{\mathbf{k}j\varepsilon}$  to zeroth order can be approximated by their values at the middle between each pair of points. In this way, the integral is replaced by the discrete sum over internal grid  $\varepsilon_i$  defined for each frequency  $\omega$ . To deal with the strong momentum dependence of  $1/(\omega + \epsilon_{\mathbf{k}j\varepsilon}^s - \epsilon_{\mathbf{k}j'\varepsilon^+}^{s'})$ , linearization of the denominator with respect to  $\mathbf{k}$  should be performed as it is done in the tetrahedron method of Lambin and Vigneron.<sup>13</sup> On the other hand, the difference between single poles [expression in square brackets of Eq. (7)], after integration over frequency, becomes a smooth function of  $\mathbf{k}$  and can be treated together with the current matrix elements,

i.e., by linearizing the numerator. The described procedure produces a fast and accurate algorithm for evaluating the optical response functions of a strongly correlated material.

### III. APPLICATION OF THE METHOD

To illustrate the method of the optical conductivity calculation in a strongly correlated system we chose paramagnetic doped Mott insulator  $\text{La}_{1-x}\text{Sr}_x\text{TiO}_3$ . LDA cannot reproduce insulating behavior of this system already at  $x=0$ , which emphasizes the importance of correlation effects. Upon doping the system becomes a correlated metal, which at  $x=1$  ( $\text{SrTiO}_3$ ) should be considered as a standard band insulator. Photoemission experiments<sup>14</sup> as a function of doping display both a lower Hubbard band located at near energies 2 eV below the Fermi level  $E_F$  and a quasiparticle band centered at  $E_F$ . Previous DMFT based calculations<sup>5,15</sup> of the density of states used  $t_{2g}$  degenerate bands of Ti found near  $E_F$  and reproduced both these features with a good accuracy. The studies of the optical properties for  $\text{LaTiO}_3$  with the less accurate LDA+ $U$  method<sup>16</sup> have been also carried out.<sup>17</sup>

We have calculated the electronic structure of  $\text{La}_{1-x}\text{Sr}_x\text{TiO}_3$  using the LDA+DMFT method. A cubic crystal structure with five atoms per unit cell is utilized which is a simplified version of a fully distorted 20 atoms/cell superlattice. Since the self-energy effects are crucial for the states near the Fermi energy, we treat correlations only on the downfolded  $t_{2g}$  orbitals of Ti atoms as suggested previously.<sup>5,15</sup> The Anderson impurity model is solved using quantum Monte Carlo method with Hubbard parameter  $U = 6$  eV at  $T = 1/\beta = 1/32$  of Ti  $t_{2g}$  bandwidth, which delivers the self-energy  $\Sigma(\omega)$  for these orbitals using the self-consistent DMFT framework. The applicability of QMC is justified since temperature in our simulation is well below the coherence energy, which is about 1/8 of the bandwidth. We also limit our consideration by dopings  $x$  larger than 10 per cent to stay below the coherence temperature. Once the self-energy is obtained, we unfold it back into the full orbital space which delivers the one-electron spectrum of the system with correlation effects taken into account. Detailed description of downfolding/upfolding procedures to get the self-energy is given in the Appendix.

To treat doping away from  $x=0$  the self-energy is allowed to change self-consistently while the one-electron Hamiltonian is assumed to be independent on doping. We then evaluate the frequency-dependent eigenvalues  $\epsilon_{\mathbf{k}j\omega}$ ,  $\psi_{\mathbf{k}j\omega}$  as functions of doping. This allows us to evaluate the energy and doping dependent optical conductivity integrals both in  $\mathbf{k}$  and  $\epsilon$  spaces. The integrals over momentum are taken on the (10, 10, 10) mesh using the tetrahedron method of Ref. 13. To check the convergence we also performed the calculations on the (6,6,6) mesh which produces the conductivity within 5% of accuracy. The energy-integration mesh was chosen to have a step equal to 0.01 eV. We also broaden the imaginary part of the self-energy for noninteracting bands with 0.0004 eV. This reproduces the LDA density of states of the studied compound within the accuracy of 1–2 %.

We first discuss the undoped case with  $x=0$  which corresponds to the insulator with a small gap equal to 0.2–0.5 eV.

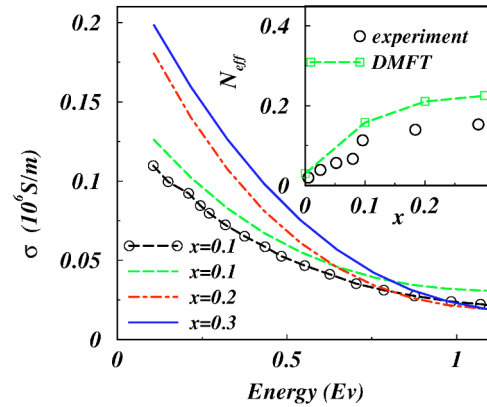


FIG. 1. (Color online) Low-frequency behavior of the optical conductivity for  $\text{La}_{1-x}\text{Sr}_x\text{TiO}_3$  at  $x=0.1, 0.2, 0.3$  calculated using the LDA+DMFT method. Experimental results (Ref. 19) are shown by symbols for the case  $x=0.1$ . In the inset the effective number of carriers is plotted as a function of doping. Squares show the results of the LDA+DMFT calculations. Circles denote the experimental data from Ref. 19.

Model calculations for threefold degenerate Hubbard model, used to get the self-energy for Ti  $t_{2g}$  bands, produce a Mott-Hubbard gap equal to 2.8 eV but once unfolded into the LDA Hamiltonian one needs to take into account La  $5d$  states in the vicinity of the Fermi level. The gap between the lower Hubbard band and La  $5d$  bands is indeed the charge-transfer gap and it is equal to 0.2–0.5 eV for the undoped compound. Optical transitions from the lower Hubbard band to La  $5d$  give the main contribution to the optical conductivity in pure  $\text{LaTiO}_3$ .

Upon doping, carriers are introduced, and the system exhibits metallic behavior. Figure 1 shows low-frequency part of  $\sigma_{xx}(\omega)$  at dopings  $x=0.1, 0.2$ , and  $0.3$ . The optical conductivity exhibits a Drude peak whose strength is increased with doping. The contribution to  $\sigma_{xx}(\omega)$  at these frequencies is due to transitions from (i) the coherent part of the spectrum near the Fermi level to the upper Hubbard and lanthanum bands, (ii) the transitions from the lower Hubbard band to the upper Hubbard band and lanthanum bands, and (iii) transitions from the lower Hubbard band to the coherent part of the spectra. This trend correctly reproduces the optical-absorption experiments performed for  $\text{La}_{1-x}\text{Sr}_x\text{TiO}_3$ .<sup>18</sup> Comparison of our data with these measurements is shown in Fig. 1, where the measured optical conductivity at the doping level  $x=0.1$  is plotted by symbols. Overall good agreement can be found for the frequency behavior of the theoretical and experimental curves.

The strength of the Drude peak is only slightly overestimated by the present theory as well as some residual discrepancy is seen in the region near 1 eV. We must emphasize that corresponding calculations based on the local-density approximation would completely fail to reproduce the doping behavior due to the lack of the insulating state of the parent compound  $\text{LaTiO}_3$ . As a result, the LDA predicts a very large Drude peak even for  $x=0$ , which remains *little changed* as a function of doping. In view of these data, the correct trend upon doping captured by the present calculation as well as proper frequency behavior can be considered as a significant

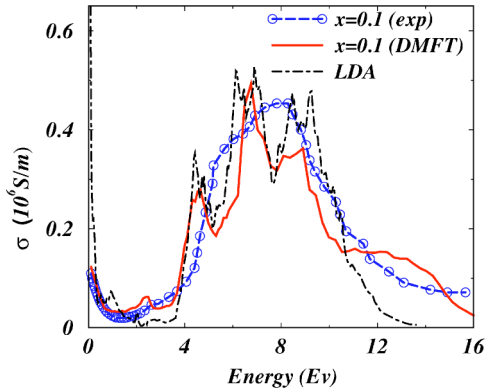


FIG. 2. (Color online) Calculated using the DMFT optical conductivity spectrum for  $\text{La}_x\text{Ti}_{1-x}\text{O}_3$  with  $x=0.1$  at large frequency interval (solid line) as compared with the experimental data (dashed line with symbols). The results of the LDA calculations are shown by dashed line.

improvement brought by this realistic DMFT study.

More insight can be gained by comparing the effective number of carriers participating in the optical transitions which is defined by  $N_{\text{eff}}(\omega_c) = (2m/\pi e^2) \int_0^{\omega_c} \sigma(\omega) d\omega$ , where  $m$  is free electron mass and  $\omega_c$  is the cutoff energy. Experimental data for  $N_{\text{eff}}(\omega_c)$  are available for the frequency  $\omega_c = 1.1$  eV.<sup>19</sup> They are shown in the inset to Fig. 1 where we plot the effective number of electrons as a function of hole concentration both from the theory and experiment.<sup>19</sup> At zero doping the system is an insulator which gives very small  $N_{\text{eff}}$  for  $x=0$  (this value is nonzero since we took  $\omega_c$  larger than the optical gap of the insulator). Upon doping, increase in  $N_{\text{eff}}$  is expected and its values as well as slope  $dN_{\text{eff}}/dx$  agree well with experiment.

The main effect introduced by the DMFT calculation on the strength of the optical transitions can be understood by looking at the Drude and interband contributions separately and comparing them with the corresponding LDA values. The LDA data give a very large  $N_{\text{eff}} = 1.15$  which by 90% consists of the Drude contribution. The latter can be found from the following equation:  $N_{\text{eff}}^D = (2mV/\pi e^2)(\omega_p^2/8)$ , where plasma frequency  $\omega_p = 4.87$  eV is obtained from LDA calculations. This result is not surprising since in LDA the  $t_{2g}$  states crossing the Fermi level are filled with one electron which gives an estimation for the effective number of electrons participating in optical transitions at this frequency range. Thus, due to proximity to the insulator the DMFT suppresses 90% of the Drude part accounted for incorrectly by the metallic LDA spectrum.

Now we discuss optical conductivity for the frequency interval from 0 to 16 eV. Figure 2 shows  $\sigma_{xx}(\omega)$  at doping  $x=0.1$  where we compare our DMFT and LDA calculations with the measurements in Ref. 18. Sharp increase in optical conductivity is seen at  $\omega \sim 4$  eV. This can be attributed to the transitions from the oxygen  $p$  band into unoccupied  $d$  states of Ti. The main peak of optical transitions is located between 5 and 10 eV, which is predicted by both DMFT calculation (solid line) and the LDA (dashed line). It is compared well with the measured spectrum (dashed line with symbols). Since the self-energy corrections modify only the states near

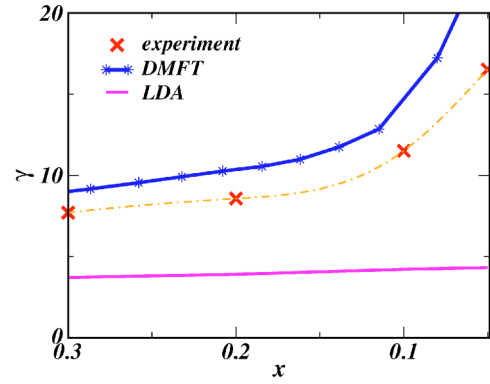


FIG. 3. (Color online) Comparison of the linear coefficient of specific heat,  $\gamma$ , as a function of doping obtained from DMFT (solid line with stars) and LDA (solid line) calculations against experimental result (Ref. 20). Experimental points are given by cross symbols and dot-dashed line is used as a guide for the eye.

the Fermi level, we do not expect DMFT spectrum to be essentially different from the LDA one in this frequency range. Overall, the agreement at high frequencies is quite good, which demonstrates reliability of the present method.

As an additional check of the DMFT calculation, we have extracted the values of the linear specific-heat coefficient  $\gamma$  as a function of doping. Our comparisons with the experiment<sup>20</sup> are given in Fig. 3. For example, at  $x=0.1$ , experimental  $\gamma = 11$  mJ/mol K<sup>2</sup>, while DMFT produces  $\gamma$  equal to 14 mJ/mol K<sup>2</sup>. Note that the LDA value here is only about 4 mJ/mol K<sup>2</sup>. Since DMFT renormalizes the density of states at the Fermi level,  $\gamma$  obtained by this theory clearly indicates the importance of band narrowing introduced by correlations.

#### IV. CONCLUSION

In conclusion, we have shown how the optical properties of a realistic strongly correlated system can be computed using recently developed DMFT based electronic structure method. We have developed a numerically tractable scheme which is reduced to evaluating dipole matrix elements as well as integrating in momentum and frequency spaces similar to the methods developed for noninteracting systems. As an application, we have studied the optical conductivity of  $\text{La}_{1-x}\text{Sr}_x\text{TiO}_3$  and found its correct dependence as a function of frequency and doping in comparison to the experiment. Our results significantly advance studies based on static mean-field approximations such as LDA.

The framework that we presented should be a good starting point for including vertex corrections. Local vertex corrections can be evaluated within DMFT (Ref. 4) while non-local ones can be incorporated by extending the calculations of Ref. 21 to the optical conductivity. This is analogous to how LDA spectra can be improved via the *GW* method.<sup>3</sup>

#### ACKNOWLEDGMENTS

This work was supported by the NSF Grant No. DMR-0096462. The authors are indebted to A. I. Lichtenstein for

valuable discussions. We also acknowledge a warm hospitality extended to three of us (V.O., G.K., and S.S.) during our stay at Kavli Institute for Theoretical Physics during the workshop “Realistic Theories of Correlated Electron Materials” where part of this work has been carried out under Grant No. PHY99-07949.

#### APPENDIX: COMPUTATION OF THE SELF-ENERGY, DMFT DOWNFOLDING, AND UPFOLDING

The approach described in Sec. II requires evaluation of the self-energy operator in Eq. (1) using the LDA+DMFT method.<sup>5</sup> The latter exploits the locality of the self-energy in some orbital space, and the restriction of the Coulomb interaction to a limited set of localized (or heavy) orbitals to be denoted by  $h$ . The rest of the orbitals are taken to be uncorrelated (light) and are denoted by  $l$ .

Note that the locality of the self-energy is a basis-dependent statement. Under a change of the basis the Kohn-Sham Hamiltonian  $H_{\mathbf{k}}$  is transformed into  $U_{\mathbf{k}} H U_{\mathbf{k}}^{\dagger}$ , with  $U_{\mathbf{k}}$  being a unitary transformation. The self-energy transforms like the Hamiltonian, however, if  $\Sigma(\omega)$  is momentum independent in one basis, then in the new basis  $\Sigma' = U_{\mathbf{k}} \Sigma(\omega) U_{\mathbf{k}}^{\dagger}$  in general becomes momentum dependent. Hence, we need to work in a very localized basis, such as the nonorthogonal LMTO's, where the DMFT approximation is most justified.

Introduction of a basis set allows the partition of the double-counting subtracted Kohn-Sham Hamiltonian  $H_{hh}^0 = H_{hh} - \Sigma_{dc}$  and of the Green's function into the light and heavy blocks:

$$G(\mathbf{k}, \omega) = \left[ (\omega + \mu) \begin{pmatrix} O_{hh} & O_{hl} \\ O_{lh} & O_{ll} \end{pmatrix}_{\mathbf{k}} - \begin{pmatrix} H_{hh}^0 & H_{hl}^0 \\ H_{lh}^0 & H_{ll}^0 \end{pmatrix}_{\mathbf{k}} - \begin{pmatrix} \Sigma_{hh}(\omega) & 0 \\ 0 & 0 \end{pmatrix} \right]^{-1}, \quad (\text{A1})$$

where  $[\dots]^{-1}$  means matrix inversion,  $\mu$  is the chemical potential, and  $O$  is the overlap matrix. Given that the self-energy is local, it can be obtained from the Anderson impurity model

$$S_{imp} = \sum_{\alpha\alpha', \tau\tau'} c_{\alpha}^{+}(\tau) \mathcal{G}_{\alpha\alpha'}^{-1}(\tau, \tau') c_{\alpha'}(\tau') + \sum_{\alpha\beta\gamma\delta, \tau} \frac{U_{\alpha\beta\delta\gamma}}{2} c_{\alpha}^{+}(\tau) c_{\beta}^{+}(\tau) c_{\gamma}(\tau) c_{\delta}(\tau), \quad (\text{A2})$$

where  $\mathcal{G}_0$  is the bath Green's function which obeys the self-consistency condition<sup>5</sup> generalized to nonorthogonal basis set:

$$G_0^{-1}(\omega) = \left( \sum_{\mathbf{k}} 1 \frac{1}{(\omega + \mu) O - H^0(\mathbf{k}) - \Sigma(\omega)} \right)_{hh}^{-1} + \Sigma_{hh}(\omega). \quad (\text{A3})$$

When a group of bands is well separated from the others, it is possible to recast the previous self-consistency condition at low frequencies in a form which resembles the DMFT equations derived from a Hamiltonian involving the  $h$  de-

grees of freedom only. In the one-electron approach it goes under the name downfolding.<sup>22</sup>

Performing standard matrix manipulations and a low-frequency expansion with linear accuracy in  $\omega$  (which is justified for low-energy calculations, provided the separation of energy scales between the band near the Fermi level and the rest) we rewrite the heavy block of the Green's function as

$$G_{hh}(\mathbf{k}, \omega) = [Z_{\mathbf{k}}^{-1} \omega - \tilde{H}(\mathbf{k}) - \Sigma_{hh}]^{-1}, \quad (\text{A4})$$

where renormalization amplitude  $Z_{\mathbf{k}}$  and effective Hamiltonian are given by

$$Z_{\mathbf{k}}^{-1} = O_{hh} + K_{hl} K_{ll}^{-1} O_{ll} K_{ll}^{-1} K_{lh} - O_{hl} K_{ll}^{-1} K_{lh} - K_{hl} K_{ll}^{-1} O_{lh},$$

$$\tilde{H}(\mathbf{k}) = H_{hh}^0 - K_{hl} K_{ll}^{-1} K_{lh},$$

$$K_{\gamma} = H_{\gamma}^0 - \mu O_{\gamma}. \quad (\text{A5})$$

Here  $\gamma$  stands for a pair of indices  $l$  or  $h$ . Finally, we perform a unitary transformation  $S$  in the heavy block, so as to work in a nearly orthogonal basis in the  $h$  sector:

$$S^{\dagger} \left[ \sum_{\mathbf{k}} Z_{\mathbf{k}} \right]^{-1} S = 1. \quad (\text{A6})$$

Applying this transformation to Eq. (A5) we arrive to the local Green's function in the new basis,

$$G_{hh}(\omega) = \sum_{\mathbf{k}} [(\omega + \mu) O_{eff}(\mathbf{k}) - H_{eff}(\mathbf{k}) - \Sigma(\omega)]^{-1}, \quad (\text{A7})$$

and to a new DMFT self-consistency condition

$$\mathcal{G}_{0hh}^{-1}(\omega) = G_{hh}^{-1} + \Sigma(\omega). \quad (\text{A8})$$

This set of equations has clearly the form of the DMFT equations of a model involving heavy electrons only, with a Hamiltonian and an overlap matrix:

$$O_{eff}(\mathbf{k}) = S^{\dagger} Z_{\mathbf{k}}^{-1} S, \quad (\text{A9})$$

$$H_{eff}(\mathbf{k}) = S^{\dagger} \tilde{H}(\mathbf{k}) S + \mu O_{eff}(\mathbf{k}). \quad (\text{A10})$$

The self-energy  $\Sigma$  is still computed from the Anderson impurity model, but the Coulomb interaction of this model is renormalized to a smaller effective interaction  $U_{eff}$  matrix,

$$U'_{eff, \alpha' \beta' \gamma' \delta'} = \sum_{\alpha\beta\gamma\delta} [\sqrt{Z}]_{\alpha' \alpha} [\sqrt{Z}]_{\beta' \beta} [\sqrt{Z}]_{\gamma' \gamma} [\sqrt{Z}]_{\delta' \delta} U_{\alpha\beta\gamma\delta}. \quad (\text{A11})$$

Until now the discussion is general, and applies to any system where there is a set of bands well separated from the rest. Further simplifications are possible, if we assume that the system has cubic symmetry and that the overlap  $O_{eff}$  is the unit matrix. For  $d$  electrons, cubic symmetry makes the self-energy and local Green's function diagonal. In this case the momentum sum in Eq. (A7) can be replaced by the integral over energy. The local Green's function can be calculated as a Hilbert transformation,

$$G(\omega) = \int_{-\infty}^{+\infty} d\varepsilon \frac{D(\varepsilon)}{\omega + \mu - \Sigma(\omega) - \varepsilon}. \quad (\text{A12})$$

Here,  $D(\varepsilon)$  is the density of states of the reduced Hamiltonian  $H_{eff}(\mathbf{k})$ . Note that the cubic symmetry keeps  $U_{eff}$  diagonal if the bare Coulomb matrix  $U$  has that property.

Upfolding is a procedure which is “inverse” to the downfolding described above. One simply converts the self-energy  $\Sigma$  obtained from the DMFT calculation into the block self-energy  $\Sigma_{hh} = S\Sigma S^\dagger$ , which is to be inserted to the original LDA Hamiltonian, in order to compute the local Green’s function  $G(\omega)$ .

In general, the downfolded density of states  $D(\varepsilon)$  obtained from  $H_{eff}$  has a nonzero first energy moment and depends in a nonlinear way on the value of the double-counting correction, as well as on the chemical potential which enters the formulation of the original problem containing all electronic bands. Furthermore, the value of the chemical potential in the LDA+DMFT calculations does not need to be the same as the LDA value.

The reduction of the self-consistent LDA+DMFT equations to the form described by Eq. (A12) with  $D(\varepsilon)$  being the partial LDA density of states of the heavy orbitals was suggested and used in Ref. 23. Unfortunately, this partial density of states contains weight at high energies, and if this is omitted, the normalization condition is violated. The derivation presented in this appendix eliminates these difficulties, and instead suggests an alternative procedure in which we first carry out a tight-binding fit of the LDA bands (downfolding) near the Fermi level, and then use it to estimate  $D(\varepsilon)$ . Our derivation also indicates how one goes back (i.e., upfolds the self-energy) to the all-orbital Hamiltonian. In our calculations using the downfolded equations  $\mu$  was adjusted to get the correct density of  $d$  electrons. In the upfolded Green’s function  $\mu$  was taken to be the LDA chemical potential, and  $\Sigma_{dc}$  was deduced from a constant shift of the heavy orbitals by obtaining the total number of electrons from the integral of the spectral function

$$A(\omega) = -\frac{1}{\pi} \text{Im} \sum_{\mathbf{k}} \sum_{\alpha\beta} G_{\alpha\beta}(\mathbf{k}, \omega) O_{\alpha\beta}^{\mathbf{k}},$$

multiplied by the Fermi function.

---

<sup>1</sup>For a review, see, e.g., *Theory of the Inhomogeneous Electron Gas*, edited by S. Lundqvist and S. H. March (Plenum, New York, 1983).  
<sup>2</sup>See, e.g., E. G. Maksimov, I. I. Mazin, S. N. Rashkeev, and Y. A. Uspenski, *J. Phys. F: Met. Phys.* **18**, 833 (1988).  
<sup>3</sup>For a review, see G. Onida, L. Reining, and A. Rubio, *Rev. Mod. Phys.* **74**, 601 (2002).  
<sup>4</sup>For a review, see, e.g., A. Georges, G. Kotliar, W. Krauth, and M. J. Rozenberg, *Rev. Mod. Phys.* **68**, 13 (1996).  
<sup>5</sup>V. I. Anisimov, A. I. Poteryaev, M. A. Korotin, A. O. Anokhin, and G. Kotliar, *J. Phys.: Condens. Matter* **9**, 7359 (1997).  
<sup>6</sup>A. I. Lichtenstein, M. I. Katsnelson, and G. Kotliar, *Phys. Rev. Lett.* **87**, 067205 (2001).  
<sup>7</sup>K. Held, A. K. McMahan, and R. T. Scalettar, *Phys. Rev. Lett.* **87**, 276404 (2001).  
<sup>8</sup>S. Y. Savrasov, G. Kotliar, and E. Abrahams, *Nature (London)* **410**, 793 (2001).  
<sup>9</sup>G. Kotliar and S. Savrasov, in *New Theoretical Approaches to Strongly Correlated Systems*, edited by A. M. Tsvelik (Kluwer Academic, The Netherlands, 2001), p. 259; S. Y. Savrasov and G. Kotliar, *Phys. Rev. B* **69**, 245101 (2004).  
<sup>10</sup>J. E. Hirsch and R. M. Fye, *Phys. Rev. Lett.* **56**, 2521 (1986).  
<sup>11</sup>O. K. Andersen, *Phys. Rev. B* **12**, 3060 (1975).  
<sup>12</sup>G. D. Mahan, *Many-Particle Physics*, 2nd ed. (Plenum, New

York, NY, 1993).  
<sup>13</sup>Ph. Lambin and J. P. Vigneron, *Phys. Rev. B* **29**, 3430 (1984).  
<sup>14</sup>A. Fujimori, I. Hase, M. Nakamura, H. Namatame, Y. Fujishima, Y. Tokura, M. Abbate, F. M. F. de Groot, M. T. Czyzyk, J. C. Fuggle, O. Strebel, F. Lopez, M. Domke, and G. Kaindl, *Phys. Rev. B* **46**, 9841 (1992).  
<sup>15</sup>I. A. Nekrasov, K. Held, N. Bluemer, A. I. Poteryaev, V. I. Anisimov, and D. Vollhardt, *Eur. Phys. J. B* **18**, 55 (2000).  
<sup>16</sup>For a review, see V. I. Anisimov, F. Aryasetiawan, and A. I. Lichtenstein, *J. Phys.: Condens. Matter* **9**, 767 (1997).  
<sup>17</sup>I. Solovyev, N. Hamada, and K. Terakura, *Phys. Rev. B* **53**, 7158 (1996).  
<sup>18</sup>Y. Fujishima, Y. Tokura, T. Arima, and S. Uchida, *Phys. Rev. B* **46**, 11167 (1992).  
<sup>19</sup>Y. Okimoto, T. Katsufuji, Y. Okada, T. Arima, and Y. Tokura, *Phys. Rev. B* **51**, 9581 (1995).  
<sup>20</sup>K. Kumagai, T. Suzuki, Y. Taguchi, Y. Okada, Y. Fujishima, and Y. Tokura, *Phys. Rev. B* **48**, 7636 (1993).  
<sup>21</sup>P. Sun and G. Kotliar, *Phys. Rev. Lett.* **92**, 196402 (2004).  
<sup>22</sup>O. K. Andersen and T. Saha-Dasgupta, *Phys. Rev. B* **62**, R16219 (2000), and references therein.  
<sup>23</sup>K. Held, I. A. Nekrasov, N. Blümer, V. I. Anisimov, and D. Vollhardt, *Int. J. Mod. Phys. B* **15**, 2611 (2001).